Hydrogen-Bond Topology and the Ice VII/VIII and Ice I*h*/XI Proton-Ordering Phase Transitions

Sherwin J. Singer,[1] Jer-Lai Kuo,[1,2,3] Tomas K. Hirsch,[4,*] Chris Knight,[1] Lars Ojamäe,[5] and Michael L. Klein[2]

[1]*Department of Chemistry, The Ohio State University, Columbus, Ohio 43210, USA*
[2]*Center for Molecular Modeling, University of Pennsylvania, Philadelphia, Pennsylvania 19104, USA*
[3]*School of Physical and Mathematical Sciences, Nanyang Technological University, Singapore 637616, Republic of Singapore*
[4]*Physical Chemistry, Arrhenius Laboratory, Stockholm University, SE-106 91 Stockholm, Sweden*
[5]*Department of Chemistry, IFM, Linköping University, SE-581 83 Linköping, Sweden*

(Received 2 October 2004; published 7 April 2005)

The existence of an ice I*h*/XI proton-ordering transition to a low-temperature ferroelectric phase has sparked considerable debate in the literature. Electronic density functional theory calculations, extended using graph invariants, confirm that a transition to a low-temperature ferroelectric phase should occur. The predicted transition at 98 K is in qualitative agreement with the observed transition at 72 K, and the low-temperature phase is the ferroelectric phase determined in diffraction experiments. The theoretical methods used to predict the phase transition are validated by comparing their prediction to the well-characterized ice VII/VIII proton-ordering transition.

DOI: 10.1103/PhysRevLett.94.135701 PACS numbers: 64.60.Cn, 02.10.Ox

In 1935 Pauling [1] estimated there are $(3/2)^N$ different ways to arrange the hydrogen bonds (H bonds) of N water molecules in an ice-I*h* lattice, ''ordinary ice,'' as illustrated in Fig. 1. Pauling's estimate proved to be remarkably accurate, the exact result [2] being $(1.5069)^N$. In the following year, Giauque and Stout measured the entropy of ice I*h* at 0 K to be $Nk_B \ln\frac{3}{2}$ within experimental error [3], implying that somewhere between 0 °C and 0 K ordinary ice becomes a proton glass with a quenched, nearly random, arrangement of H bonds. Since that time there has been continued research and debate as to whether the H-bond arrangements are indeed completely random and whether there lurks a phase transition to a fully proton-ordered form of ice I*h*. Recently, ''spin ice'' materials have been found in which magnetic moments obey the same configurational constraints as H bonds in ice and exhibit a similar $Nk_B \ln\frac{3}{2}$ residual entropy [4]. Similar issues concerning phase transitions to fully ordered structures arise for spin ices, and our graph invariant method [5,6] of harnessing electronic density functional theory (DFT) techniques to formulate an accurate statistical mechanical treatment of H-bond fluctuations may well find application in this area.

There is a calorimetric signature of a first-order phase transition in KOH-doped ice I*h*, weakly dependent on KOH concentration and tending toward 72 K in the limit of vanishing impurity concentration [7,8]. Presumably hydroxide ions catalyze H-bond rearrangement and enable approach to equilibrium. Neutron scattering [9–12] and thermal depolarization experiments [13,14] on KOH-doped ice I*h* suggest that the proton-ordered form of ice I*h*, known as ice XI, is an orthorhombic ferroelectric crystal. This view has been contested. Lately, Iedema *et al.* [15] referred to more recent claims as ''UFI citings (under-identified ferroelectric ices) in the literature.''

In contrast, the ice VII/VIII proton-ordering transition is well characterized and serves as a test case for our theoretical methods. The ice VII/VIII structure consists of two interpenetrating ice I*c* lattices. Over a range of pressures from 2.1 to 12 GPa, proton ordering via H-bond rearrangements occurs at nearly constant temperature, variously reported [16,17] from 263 to 273 K. With still higher pressure, the ice VII/VIII transition temperature abruptly decreases as the mechanism of the transition shifts to proton tunneling across the shortened H bonds. Our calculations are pertinent to the temperature independent region.

In this work we show that electronic density functional theory gives a robust description of the energetics of the H-bond isomers and, coupled with an analytic method we have developed [5,6], provides new insight into proton ordering in ice. These techniques are validated for the ice VII/VIII transition and then applied to the I*h*/XI transition. Prediction of H-bond ordering in ice encounters several obstacles. Buch, Sandler, and Sadlej [18] showed that empirical potentials disagree among each other with regard to the subtle energetic ordering of the H-bond isomers in ice I*h* and differed by an order of magnitude with respect to

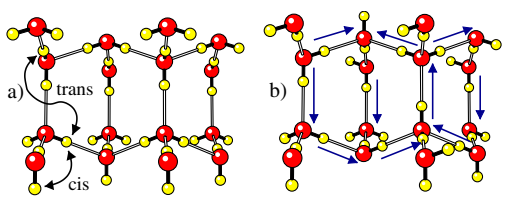

FIG. 1 (color online). Two possible arrangements of H bonds within a 16-water unit cell of ice I*h*. The possible H-bond isomers are summarized mathematically by directed graphs in which directional bonds point from H-bond donor to H-bond acceptor, as illustrated for an isomer (b).

the range of energy differences. None of the empirical potentials predicted the ground state to be the $Cmc2_1$ crystal structure suggested by diffraction data, including a potential they constructed with that hope in mind. We overcome this problem through electronic DFT calculations. Then, we solve the problem of statistical sampling of H-bond configurations by linking energy to hydrogen-bond topology using *graph invariants* [5,6], combinations of H-bond variables which are invariant to space group symmetry operations that are appropriate variables for describing scalar physical properties. Graph invariants provide a means to "bootstrap" from expensive DFT calculations for smaller unit cells to statistical mechanical simulations using a larger unit cell.

The H-bond network is summarized mathematically by oriented graphs, vertices connected by directed lines (Fig. 1). The direction of the ith H bond in the ice lattice is specified by a bond variable b_i which takes values ± 1 according to whether the bond points along or opposite to a canonical direction for that bond. If a scalar physical property, such as the energy, can be predicted on the basis of the H-bond topology, it must depend on the bond variables in combinations which are invariant to symmetry operations g_α of the space group [5,6]. These combinations are generated by the action of the projection operator for the totally symmetric representation on bond variables $I_i \propto \sum_\alpha g_\alpha(b_i)$ (first-order invariants), products of two bond variables $I_{ij} \propto \sum_\alpha g_\alpha(b_i b_j)$ (second-order invariants), and so on. Assuming the simplest linear dependence, the energy is written as

$$E(b_1, b_2, \ldots) = E_0 + \sum_r \alpha_r I_r + \sum_{rs} \alpha_{rs} I_{rs} + \cdots, \quad (1)$$

with the overall constant E_0 and the α coefficients to be determined either by comparison with experiment, or as we do in this work, by first-principles calculation. In a bootstrap strategy, we perform expensive electronic structure calculations on relatively small unit cells to determine the α coefficients and then evaluate expression (1) for the many H-bond isomers of a larger unit cell to generate a statistical average. Technical aspects of generating graph invariants for periodic lattices have been addressed elsewhere [5]. For systems possessing sufficient symmetry the first-order invariants are identically zero, and second-order invariants provide the leading order link between H-bond topology and physical properties.

We have already demonstrated [6] how graphical techniques can be used to understand and predict physical properties of water clusters. Long ago, Bjerrum [19] suggested that H bonds in ice break into two categories, depending on whether the nonhydrogen bonded hydrogens are in a trans or cis arrangement, that is, whether they fall on opposite or the same sides of the H bond. Examples of waters in trans and cis arrangements are indicated in Fig. 1. The number of trans bonds is actually an example of an invariant. The presumed dominance of pairwise interactions has led to proposals that ice structures with the highest fraction of trans H bonds are most stable [19], a notion that, if correct, would conflict with the proposed ferroelectric structure of ice XI in which three-quarters of the H bonds are cis. Nevertheless, the cis or trans example does serve to illustrate how a graph invariant can be used to extrapolate from electronic structure calculations for small unit cells to the large unit cells needed for statistical simulations: The cis or trans energy difference is a parameter that can be determined from rather small unit cells [20]. *If* the relative number of cis and trans H bonds did control the energy, then the energy of the myriad H-bond arrangements of a large cell would be known by counting the relative number of cis and trans H bonds in each of those configurations. Our results indicate there are other important features, described by further invariants, which link scalar physical properties to H-bond topology in ice. The use of graph invariants provides a means to generate the full set of topological parameters in the form of invariant polynomials of bond variables b_r, and organizing them in a hierarchy of increasingly accurate approximations [5,6]. In this work we retain only the leading order, that is, second-order invariants, which will be seen to provide an accurate description of the H-bond energetics of larger ice unit cells.

Our study of the ice VII/VIII transition begins with the 16-water unit cell of ice VII, 2 primitive unit cells on each side. Periodic DFT calculations were performed using the Car-Parrinello [21] method [Becke-Lee-Yang-Parr (BLYP) functional, Γ point used to sample the Brillouin zone] on all 52 possible, symmetry-distinct H-bond isomers possible in this unit cell, enumerated using previously described methods [6,22,23]. The dependence of energy on H-bond topology was well captured by an expression of the form of Eq. (1) using only second-order invariants, quadratic polynomials in the bond variables b_r. A good fit required only those second-order invariants in which the terms $b_r b_s$ involve bonds that either had a vertex in common or were separated by a single bond. This left three graph invariants plus an overall constant [3 α coefficients plus E_0 in Eq. (1)] to describe the energy of the 52 isomers, yielding the fit shown in Fig. 2(a). The energy actually calculated for 30 randomly chosen isomers of a larger 32-water cell, measuring $2\sqrt{2} \times 2\sqrt{2} \times 2$ primitive cells on each side, is predicted well using invariant parameters from the smaller 16-water cell in Fig. 2(b), indicating we are nearing convergence of the graph invariant parameters with respect to unit cell size. However, the calculated energies systematically vary over a slightly wider range than those predicted ("bootstrapped") from the smaller cell. This is actually not a consequence of requiring more invariant parameters, but rather is due to more freedom for configurational relaxation and greater effective k-point sampling for the larger unit cell. The energies of the larger cell were fit to the same invariant parameters as the smaller

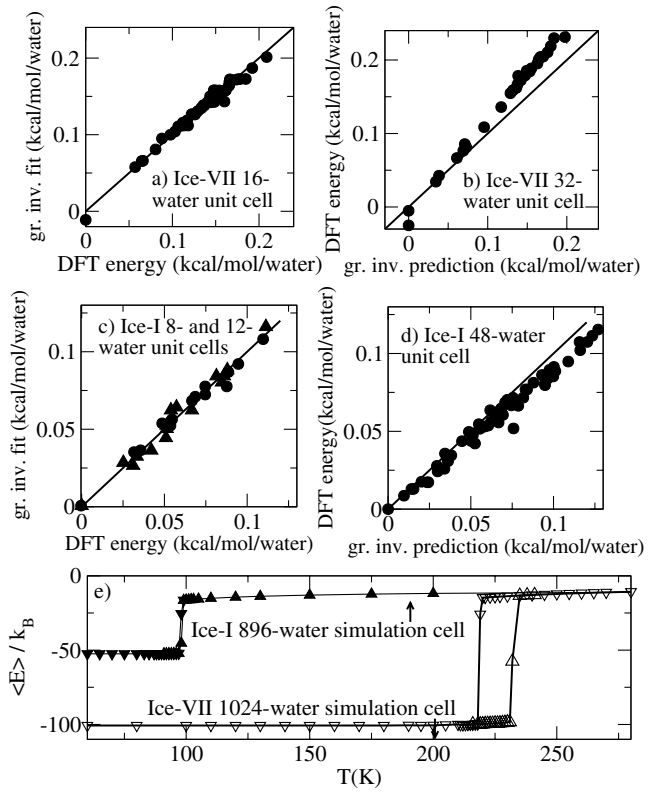

FIG. 2. (a) Graph invariant fit to the energies of the 52 H-bond isomers of a 16-water unit cell of ice VII. (b) Calculated DFT energy of H-bond isomers of a 32-water ice VII cell plotted against energies predicted from graph invariant parameters derived from the 16-water cell. (c) Graph invariant fit to the energies of the 30 H-bond isomers of 8-water orthorhombic and 12-water hexagonal unit cells of ice I*h*. (d) Calculated DFT energy of H-bond isomers of a 48-water ice-I*h* cell plotted against energies predicted from graph invariant parameters derived from the smaller cell. The DFT energies in plots (a)–(d) are calculated using the BLYP functional and the CPMD program. The atomic positions are fully optimized within unit cells whose size is fixed at the experimental value [24]. A line of slope unity is shown to indicate where points would lie for perfect agreement. (e) Average energy plotted as a function of temperature from Metropolis Monte Carlo simulations [24] for large simulation cells for ice I*h*/XI (filled symbols) and ice VII/VIII (open symbols). Data are presented for series of Metropolis Monte Carlo runs ascending (▲, △) and descending (▼, ▽) in temperature.

cell, yielding a fit equal in quality to that shown in Fig. 2(a) for the small cell. These improved invariant parameters were then used to predict the energies of a 1024-water statistical simulation cell. Metropolis Monte Carlo simulations [24] were performed for the largest cell [Fig. 2(e)]. Assuming that the vibrational free energy of the isomers is roughly the same, the Monte Carlo simulation yields a prediction of a first-order ice VII/VIII phase transition at 228 K. The transition temperature is calculated as the point of equal free energy between the two phases as determined by thermodynamic integration of the low-temperature phase from 0 K and the high-temperature phase from infinite temperature.

Despite the difficulties posed by small energy variation among H-bond isomers, our results qualitatively match the observed features of the ice VII/VIII phase transition in several respects: (i) the calculated ground state is the known ice-VIII antiferroelectric structure [23], (ii) the transition temperature is similar to the experimental transition point measured in the range 263–273 K [16,17], and (iii) there is a detectable partial ordering above the transition and a partial disordering below the transition. The calculated entropy of the transition is 91% of the ideal configurational entropy associated with H-bond disordering compared with experimentally reported values of 83% for H_2O and 91% for D_2O [16].

Further validation is available from our calculations for ice-I*h*. We performed DFT calculations using three different combinations of density functionals and basis sets for two smaller unit cells of ice-I*h*, an orthorhombic unit cell containing 8 water molecules [20] (half of the unit cells shown in Fig. 1) and a hexagonal cell with 12 waters. The number of symmetry-distinct H-bond isomers consistent with the ice rules and lattice periodicity is 16 and 14, respectively [5]. The different density functionals, basis sets, and programs, as detailed in the caption of Fig. 3 and supplementary material [24], agree well when applied to starting configurations, for which cell dimensions and molecular geometries for each isomer are exactly the same (solid curves in Fig. 3). Moreover, each method yields the $Cmc2_1$ structure as the lowest energy isomer. The isomers are arranged in order of increasing fraction of trans H bonds in Fig. 3, and it is apparent that this feature does not predict their relative energies. The dashed curves in Fig. 3 report energies after various forms of geometry optimization, determined by the capabilities of the electronic structure programs employed. For two of the methods, the atomic positions were optimized with cell dimensions fixed. Those two cases are in very good agreement. In the third method, the cell dimensions were optimized as well and, as would be expected, this case deviates further from the other two. The overall trends do not depend on the choice of density functional or the optimization method. The lowest energy isomer is the $Cmc2_1$ structure in each case. Therefore, while current empirical potentials do not give a reliable description of H-bond energetics in ice, DFT calculations provide a robust description.

The next stage is to fit Eq. (1) using the energies plotted in Fig. 3. The procedure is very similar to the one applied to the ice VII/VIII transition. The energies from small unit cells are fit to three graph invariants plus a constant [Fig. 2(c)]. These parameters are then tested by predicting energies for a larger unit cell, here a 48-water hexagonal cell, and comparing against new DFT calculations for the

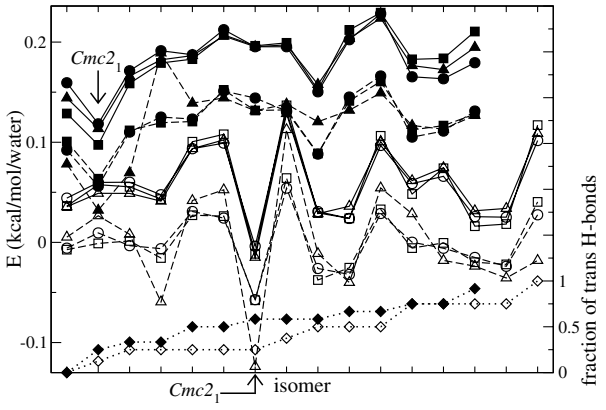

FIG. 3. Relative energy of H-bond isomers calculated by periodic electronic DFT methods for 16 isomers of an 8-water orthorhombic unit cell (open symbols) and 14 isomers of a 12-water hexagonal unit cell (filled symbols) listed in order of increasing fraction of trans H bonds. The bottom two graphs (dotted lines) give the fraction of trans H bonds associated with each isomer of the orthorhombic (◇) and hexagonal (◆) unit cells. The energy was calculated [24] using (●, ○) the BLYP functional, plane wave basis set and Troullier-Martins pseudopotentials with the CPMD program, (■, □) BLYP functional using numerical basis sets with the DMOL program, or (▲, △) the PW91 functional using plane wave basis with the CASTEP program. Solid lines: energy of H-bond isomers before geometry optimization. Dashed lines: energies after optimization of the molecular coordinates, and for the CASTEP results cell dimensions as well. The 12 energy data sets are plotted with their average taken as the zero of energy to facilitate comparison of the relative energies of the isomers. The 12 sets are broken into four groups, according to the two unit cells and whether the geometry is optimized or unoptimized. Successive groups of three curves are shifted by 0.06 kcal/mol for clarity. The $Cmc2_1$ isomers for the orthorhombic and hexagonal cells are indicated.

larger cell [Fig. 2(d)]. The predictions from the smaller cell are close to the larger one, but, again, there is a systematic deviation resulting from more freedom for geometrical relaxation and more effective k-point sampling. Parameters obtained by fitting energies calculated for 63 isomers for the 48-water cell are then used to predict the energetics of an 896-water simulation cell. Average energy as a function of temperature resulting from Monte Carlo simulations for the simulation cell, shown in Fig. 2(e), indicates a transition to the low-temperature ferroelectric $Cmc2_1$ structure at 98 K. The calculations indicate that as ice Ih is cooled, it loses 11% of its configurational entropy before the transition (in agreement with pretransitional effects seen calorimetrically [8] and in diffraction studies [12]), 88% at the Ih/XI transition, and 1% as ice XI is cooled to 0 K.

After the existence of an ice Ih/XI transition to a low-temperature ferroelectric phase has sparked considerable debate, electronic DFT calculations, extended using graph invariants confirm that a transition to a low-temperature ferroelectric phase should occur. The predicted transition at 98 K is in good agreement with the observed transition at 72 K, and the low-temperature phase is the ferroelectric phase determined in diffraction experiments.

We gratefully acknowledge support of the NSF, Swedish Research Council VR, Wenner-Gren Foundation, as well as the Ohio, Pittsburgh, SNAC, and NSC Supercomputer Centers.

*Present address: Stanford Linear Accelerator Center, Menlo Park, CA, USA.

[1] L. Pauling, J. Am. Chem. Soc. **57**, 2680 (1935).
[2] J. F. Nagle, J. Math. Phys. (N.Y.) **7**, 1484 (1966).
[3] W. F. Giauque and J. W. Stout, J. Am. Chem. Soc. **58**, 1144 (1936).
[4] S. T. Bramwell and M. J. P. Gingras, Science **294**, 1495 (2001).
[5] J.-L. Kuo and S. J. Singer, Phys. Rev. E **67**, 016114 (2003).
[6] J.-L. Kuo, J. V. Coe, S. J. Singer, Y. B. Band, and L. Ojamäe, J. Chem. Phys. **114**, 2527 (2001).
[7] S. Kawada, J. Phys. Soc. Jpn. **32**, 1442 (1972).
[8] Y. Tajima, T. Matsuo, and H. Suga, Nature (London) **299**, 810 (1982).
[9] R. Howe and R. W. Whitworth, J. Chem. Phys. **90**, 4450 (1989).
[10] S. M. Jackson, V. M. Nield, R. W. Whitworth, M. Oguro, and C. C. Wilson, J. Phys. Chem. B **101**, 6142 (1997).
[11] A. J. Leadbetter, R. C. Ward, J. W. Clark, P. A. Tucker, T. Matsuo, and H. Suga, J. Chem. Phys. **82**, 424 (1985).
[12] C. M. B. Line and R. W. Whitworth, J. Chem. Phys. **104**, 10 008 (1996).
[13] S. M. Jackson and R. W. Whitworth, J. Chem. Phys. **103**, 7647 (1995).
[14] S. M. Jackson and R. W. Whitworth, J. Phys. Chem. B **101**, 6177 (1997).
[15] M. J. Iedema, M. J. Dresser, D. L. Doering, J. B. Rowland, W. P. Hess, A. A. Tsekouras, and J. P. Cowin, J. Phys. Chem. B **102**, 9203 (1998).
[16] G. P. Johari, A. Lavergne, and E. Whalley, J. Chem. Phys. **61**, 4292 (1974); **73**, 4150(E) (1980).
[17] W. F. Kuhs, J. L. Finney, C. Vettier, and D. V. Bliss, J. Chem. Phys. **81**, 3612 (1984).
[18] V. Buch, P. Sandler, and J. Sadlej, J. Phys. Chem. B **102**, 8641 (1998).
[19] N. Bjerrum, Science **115**, 386 (1952).
[20] T. K. Hirsch and L. Ojamäe, J. Phys. Chem. B **108**, 15 856 (2004).
[21] R. Car and M. Parrinello, Phys. Rev. Lett. **55**, 2471 (1985).
[22] S. McDonald, L. Ojamäe, and S. J. Singer, J. Phys. Chem. A **102**, 2824 (1998).
[23] J.-L. Kuo and M. L. Klein, J. Phys. Chem. B **108**, 19 634 (2004).
[24] See EPAPS Document No. E-PRLTAO-94-014515 for details regarding the periodic DFT and Metropolis Monte Carlo calculations. A direct link to this document may be found in the online article's HTML reference section. The document may also be reached via the EPAPS homepage (http://www.aip.org/pubservs/epaps.html) or from ftp.aip.org in the directory /epaps/. See the EPAPS homepage for more information.